18th International Conference
ENGINEERING MECHANICS 2012
Svratka, Czech Republic, May 14 – 17, 2012

pp. 211–222
Paper #92

LATTICE MODELING OF CONCRETE FRACTURE INCLUDING THE EFFECT OF MATERIAL SPATIAL RANDOMNESS

J. Eliáš [*], **M. Vořechovský** [**]

Abstract: *The paper presents stochastic discrete simulations of concrete fracturing. The spatial material randomness of local material properties is introduced into a discrete lattice-particle model via an autocorrelated random field generated by the Karhunen–Loève expansion method. The stochastic discrete model is employed to simulate failure of three-point-bent beams with and without a central notch notch. The effect of spatial randomness on the peak load and energy dissipation is studied.*

Keywords: ***lattice model, concrete, fracture, stochastic simulations, material randomness, fracture energy, flexural failure.***

1. Introduction

It has been widely recognized that mechanical properties of materials exhibit a spatial variability. The seminal theory of Weibull (1939) offered simple and powerful tool to determine the probabilistic distribution of structural strength. However, applicability of the Weibull theory is limited to brittle structures with no redistribution prior to the peak load. The Weibull theory lacks any length scale and rupture of infinitely small volume directly causes failure of the whole structure. The absence of any characteristic length scale also results in spurious infinite strength of infinitely small structures (Vořechovský, 2010). Moreover, the Weibull theory assumes that strength of every material point is independent of its surroundings. However, many structures are made of quasibrittle materials like concrete, ceramics, rocks or ice. These structures have the ability to partially redistribute released stresses and thus their failure is triggered by rupture of some representative volume of finite size. Also the Weibull assumption of independence stands out against the natural expectation that the local strength fluctuate rather continuously inside a structure.

The advantage of Weibull theory comes from the fact that the mechanics of failure does not interact with the stochastic model – only elastic stress field is needed. Extension of the Weibull theory for finite internal material length scale requires knowledge of changes in the stress field during the redistribution prior to the peak load. The redistribution can be mimicked by the nonlocal Weibull theory of Bažant and Xi (1991) and Bažant and Novák (2000), where probability of failure of material point depends not only on its local stress but also on stress in its surroundings. Therefore, local stress is replaced by nonlocal stress obtained by nonlocal averaging of the (local) elastic stress field (Bažant and Jirásek, 2002). The nonlocal Weibull theory agrees for the large sizes with the local one. For intermediate structural sizes, it predicts higher strengths than the local Weibull theory thanks to possible stress redistribution. Unfortunately, in the in the case of very small structures, the theory is not applicable because the approximation or stress redistribution by nonlocal averaging is too simplistic. Though the nonlocal averaging helps to introduce the material internal length, it is not able to correctly reflect possible spatial correlations of local material properties.

A laborious option of structural strength estimation is represented by stochastic failure simulations that include proper mechanics of stress redistribution. Such a stochastic analysis can be performed using the finite element method with a sophisticated material constitutive law (Vořechovský, 2007;

[*]Ing. Jan Eliáš, Ph.D.: Institute of Structural Mechanics, Faculty of Civil Engineering, Brno University of Technology, Veveří 331/95; 602 00, Brno; CZ, e-mail: elias.j@fce.vutbr.cz
[**]Doc. Ing. Miroslav Vořechovský, Ph.D.: Institute of Structural Mechanics, Faculty of Civil Engineering, Brno University of Technology, Veveří 331/95; 602 00, Brno; CZ, e-mail: vorechovsky.m@fce.vutbr.cz

Vořechovský and Sadílek, 2008). Failure of highly heterogeneous materials can also be advantageously modeled via discrete models. These models can be *deterministic*: Grassl and Rempling (2008); Van Mier and Van Vliet (2003); Bolander and Saito (1998) or *stochastic*: Grassl and Bažant (2009); Alava et al. (2006). In this study, we adopt the lattice particle-model developed by G. Cusatis (Cusatis and Cedolin, 2007) for modeling of concrete fracturing. Spatial material fluctuations are introduced by modeling the material properties as realizations of a random field.

The following Section 2. briefly describes the deterministic mechanical (lattice) model and Section 3. elucidates how the spatial randomness is incorporated into the model. The model is then used for numerical simulations of failure of notched and unnotched three-point bent beams. The results are presented in Sections 4. (notched beams) and 5. (unnotched beams).

2. Deterministic model

Modeling of the initiation and propagation of cracks in quasibrittle materials exhibiting strain softening has been studied for several decades. Although this is a difficult task complicated by the distributed damage dissipating energy within a fracture process zone (FPZ) of non-negligible size, realistic results have been achieved by several different approaches; see e.g. Bažant and Planas (1998). The present study is based on the cohesive crack model (Barenblatt, 1962; Hillerborg et al., 1976; Bažant and Planas, 1998) called sometimes the fictitious crack model. It relies on an assumption that the cohesive stress transmitted across the crack is released gradually as a decreasing function of the crack opening, called the cohesive softening curve. Its main characteristic is the total fracture energy, G_F – a material constant representing the area under the softening curve.

In heterogeneous materials, the dissipation of energy takes place within numerous meso-level cracks inside the FPZ. Direct modeling of such distributed cracking calls for representation of the material meso-level structure. Models capable to efficiently incorporate the concrete meso-structure should be used. For this purpose, the present analysis will be based on the discrete lattice-particle developed by Cusatis and Cedolin (2007), which is an extension of Cusatis et al. (2003, 2006).

The material is represented by a discrete three-dimensional assembly of rigid cells. The cells are created by tessellation according to pseudo-random locations and radii of computer generated aggregates/particles. Every cell contains one aggregate (Fig. 1a,b). The cells are interconnected by set of three nonlinear springs (normal - n and two tangential - t_1, t_2) placed at the interfaces between the cells, representing the mineral aggregates in concrete and its surroundings. On the level of rigid cell connection, the cohesive crack model is used to represent cracking in the matrix between the adjacent grains. The inter-particle fracturing is assumed to be of damage-mechanics type and is modeled using a single damage variable ω applied to all three directions $i = n$, t_1 and t_2. Forces F_i in the springs can thus be evaluated from their extensions Δu_i by

$$F_i = (1 - \omega) k_i \Delta u_i \tag{1}$$

where k_i is elastic spring stiffness. The damage parameter ω depends on Δu_i and on the previous loading history of each connection. For a detailed description of the connection constitutive law or other model features, see Cusatis and Cedolin (2007). The confinement effect (present in the full version of the model) is neglected here as it was estimated that confinement does not play any important role in the studied type of experiment.

Beams of depths $D = 300$ mm, span-depth ratio $S/D = 2.4$ and thickness $t = 0.04$ m, were modeled. The maximal aggregate diameter was 9.5 mm. The minimal grain diameter was selected as 3 mm. Aggregates' diameters within the chosen range were generated using the Fuller curve. The parameters of the connection constitutive law, which were mostly taken similar to those in Cusatis and Cedolin (2007), were: matrix elastic modulus $E_c = 30$ GPa; aggregate elastic modulus $E_a = 90$ GPa; meso-level tensile strength $\sigma_t = 2.7$ MPa; meso-level tensile fracture energy $G_t = 30$ N/m; meso-level shear strength $\sigma_s = 3\sigma_t = 8.1$ MPa; meso-level shear fracture energy $G_s = 480$ N/m; meso-level compressive strength $\sigma_c = 42.3$ MPa; $K_c = 7.8$ GPa; $\alpha = 0.25$; $\beta = 1$; $\mu = 0.2$; $n_c = 2$.

To save computer time, the lattice-particle model covers only the region in which cracking was expected. Surrounding regions of the beams were assumed to remain linear elastic and were therefore

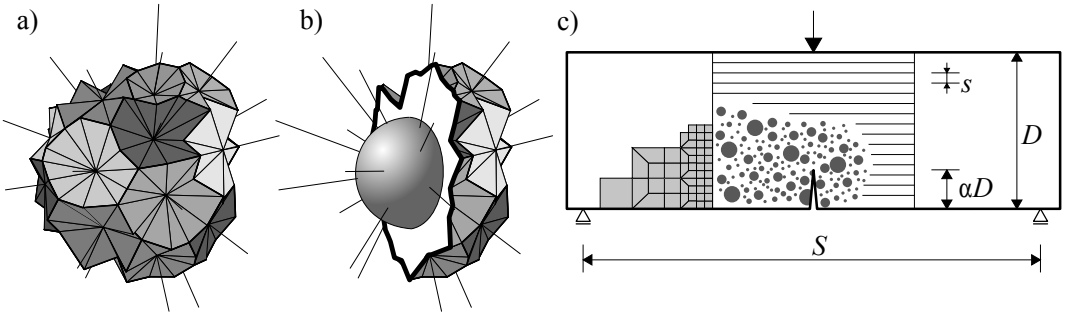

Fig. 1: a) One cell of the lattice-particle model and b) its section revealing the aggregate. c) Geometry of the beams simulated in three-point-bending.

modeled by standard 8-node isoparametric finite elements. The elastic constants for these elements were identified by fitting a displacement field with homogeneous strain to displacements of particle system subjected to low-level uniaxial compression. The macroscopic Young's modulus and Poisson ratio were found to equal $\bar{E} = 34.7$ GPa and $\bar{\nu} = 0.19$. The finite element mesh was connected to the system of particles by introducing interface nodes treated as auxiliary zero-diameter particles (Eliáš and Bažant, 2011). These auxiliary particles have their translational degrees of freedom prescribed by shape (or interpolation) functions of the nearest finite element. The rotations of the auxiliary particles were unconstrained.

3. Stochastic model

In the described discrete model, we assign material properties of each inter-particle connection according to a stationary autocorrelated random field. The value of the c-th realization of the discretized field at spatial coordinate $\boldsymbol{x}$ will be denoted $\boldsymbol{H}^c(\boldsymbol{x})$. For a given coordinate $\boldsymbol{x}_0$, $\boldsymbol{H}(\boldsymbol{x}_0)$ is a random variable H of cumulative distribution function (cdf) $F_H(h)$. Since we work with stationary random fields, the cdf $F_H(h)$ is identical for any position $\boldsymbol{x}_0$. Recent studies by Bažant and co-workers (Bažant and Pang, 2007; Bažant et al., 2009) showed that, when H represents strength of a quassibrittle material, $F_H(h)$ can be approximated by a Gaussian distribution onto which a power-law tail is grafted from the left at a probability about 10^{-4}–10^{-3}.

$$F_H(h) = \begin{cases} r_f \left(1 - e^{-\langle h/s_1 \rangle^m}\right) & 0 \le h \le h_{gr} \quad \text{(2a)} \\ F_H(h_{gr}) + \dfrac{r_f}{\delta_G\sqrt{2\pi}} \displaystyle\int_{h_{gr}}^{h} e^{-(h-\mu_G)^2/2\delta_G^2} \mathrm{d}h & h > h_{gr} \quad \text{(2b)} \end{cases}$$

where $\langle x \rangle = \max(x, 0)$, $s_1 = s_0 r_f^{1/m}$, m is the Weibull modulus (shape parameter) and s_0 is scale parameter of the Weibull tail, μ_G and δ_G are the mean value and the standard deviation of the Gaussian distribution that provides the Gaussian core. The Weibull-Gauss juncture at point at h_{gr} requires that that $(\mathrm{d}F_H/\mathrm{d}h)|_{h_{gr}^+} = (\mathrm{d}F_H/\mathrm{d}h)|_{h_{gr}^-}$. r_f is a scaling parameter normalizing the distribution to satisfy $F_H(\infty) = 1$. The distribution has in total 4 independent parameters.

The spatial fluctuation of the field is characterized through an autocorrelation function. It determines the spatial dependence pattern between the random variables at any pair of nodes. The correlation coefficient ρ_{ij} between two field variables at coordinates $\boldsymbol{x}_i$ and $\boldsymbol{x}_j$ can be assumed to obey the squared exponential function:

$$\rho_{ij} = \exp\left[-\left(\frac{\|\boldsymbol{x}_i - \boldsymbol{x}_j\|}{d}\right)^2\right] \quad (3)$$

It brings a new parameter d called the autocorrelation length.

To digitally simulate the stationary random field described by the random variable cdf F_H and correlation length d in the discrete model, we need to generate N realizations of the discretized random field $\boldsymbol{H}^0(\boldsymbol{x})$, $\boldsymbol{H}^1(\boldsymbol{x}), \ldots, \boldsymbol{H}^{N-1}(\boldsymbol{x})$ at the facet centers of the model. This is achieved using the

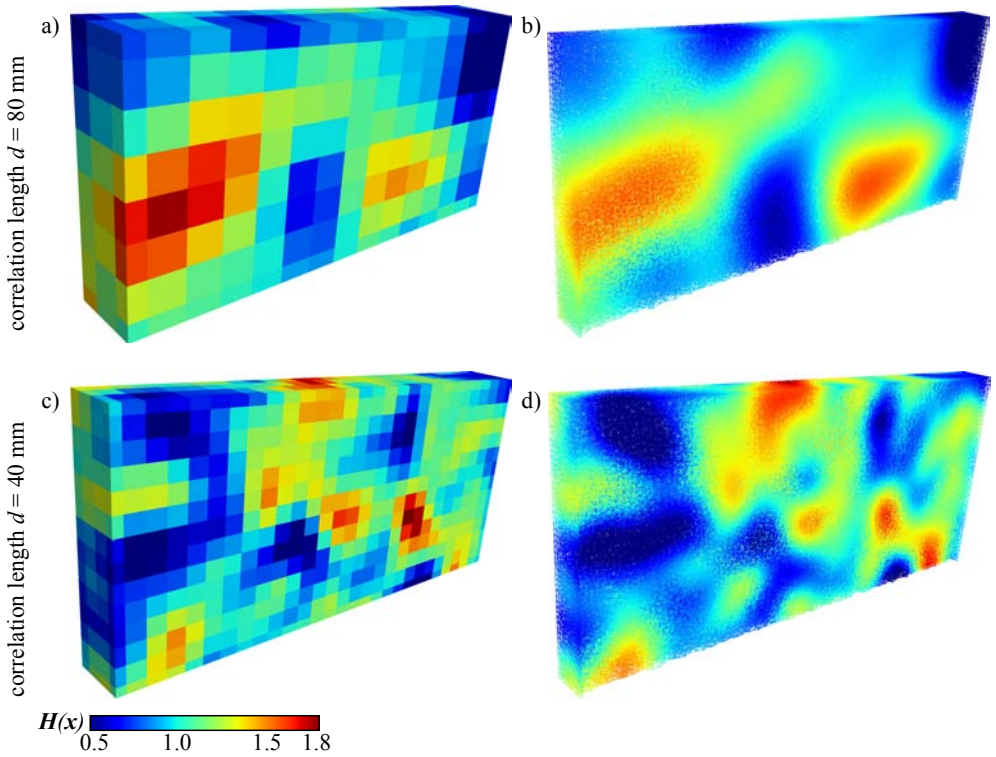

Fig. 2: Left: one realization of the autocorrelated random field $\boldsymbol{H}$ on a grid of spacing d/3 for $d = 80$ mm (top) and $d = 40$ mm (bottom). Right: realization of the field $\boldsymbol{H}$ at the element centers of the lattice-particle model.

the Karhunen–Loève expansion based on the spectral decomposition of covariance matrix $\boldsymbol{C}$, where $C_{ij} = \rho_{ij}$. This procedure decompose the correlated Gaussian variables $\widehat{\boldsymbol{H}}(\boldsymbol{x}_i)$ into independent standard Gaussian variables ξ_k that are easy to generate. $c-$th realization of the Gaussian random field $\widehat{\boldsymbol{H}}^c(\boldsymbol{x})$ is then obtained using K standard Gaussian random variables by the following expression

$$\widehat{\boldsymbol{H}}^c(\boldsymbol{x}) = \sum_{k=1}^{K} \sqrt{\lambda_k} \xi_k^c \boldsymbol{\psi}_k(\boldsymbol{x}) \tag{4}$$

where λ and $\boldsymbol{\psi}$ are the eigenvalues and eigenvectors of the covariance matrix $\boldsymbol{C}$. The value K is the number of eigenmodes/variables considered. In practice, it suffices to employ only a reduced number of eigenmodes $K \ll$ order of $\boldsymbol{C}$. In particular, K can be selected such that $\sum_{k=1}^{K} \lambda_k$ corresponds to about 99% of the trace of the covariance matrix $\boldsymbol{C}$ (Vořechovský, 2008). The vectors of independent standard Gaussian variables $\boldsymbol{\xi}$ are generated by Latin Hypercube Sampling using the mean value of each subinterval. The spurious correlation of the variables is then minimized by reordering their K realizations (Vořechovský and Novák, 2009).

A non-Gaussian random field can be generated by isoprobabilistic transformation of the underlying Gaussian field as

$$\boldsymbol{H}^c(\boldsymbol{x}) = F_H^{-1}(\Phi(\widehat{\boldsymbol{H}}^c(\boldsymbol{x}))) \tag{5}$$

Such a transformation, however, distorts the correlation structure of the field. Thus, when generating Gaussian field $\widehat{\boldsymbol{H}}$, the correlation coefficients must be modified (Vořechovský, 2008). This is here performed using the approximate method of HongShuang et al. (2008).

The realizations of the random field need to be evaluated for every shared facet (inter-particle bond) of the discrete mechanical model (at its center). This can be computationally extremely demanding for a large number of facets (large covariance matrix) and a short correlation length d (many eigenvalues needed, large K). We therefore adopted the expansion optimal linear estimation method - EOLE (Li and Kiureghian, 1993), which can significantly reduce the time of random field generation. Instead of

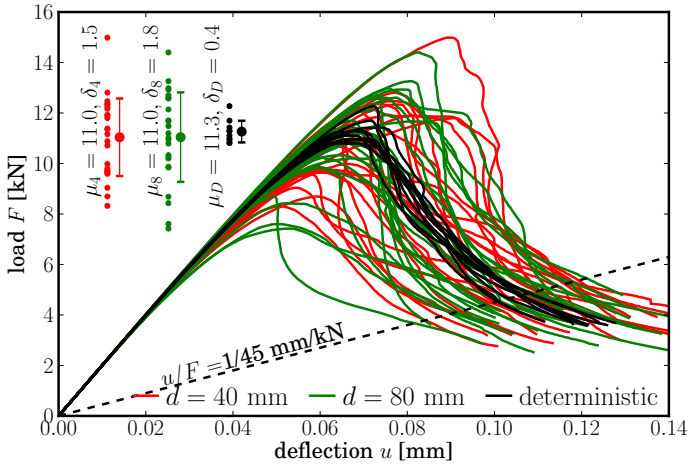

Fig. 3: Load-deflection curves for simulations of TPB beams with notch.

the facet centers, the random field is initially generated on a regular grid of nodes with spacing $d/3$ (see Fig. 2). The values of the random field at the facets are then obtain from expression

$$\widehat{\boldsymbol{H}}^c(\boldsymbol{x}) = \sum_{k=1}^{K} \frac{\xi_k^c}{\sqrt{\lambda_k}} \boldsymbol{\psi}_k^T \boldsymbol{C}_{xg} \tag{6}$$

where λ and $\boldsymbol{\psi}$ are now eigenvalues and eigenvectors of the covariance matrix of the grid nodes, and $\boldsymbol{C}_{xg}$ is a covariance matrix between facet center at coordinates $\boldsymbol{x}$ and the grid nodes. After the Gaussian random field values at facet centers are obtained by EOLE (Eq. 6), they need to be transformed to the non-Gaussian space by Eq. 5.

Besides the significant time savings, another advantage of using EOLE is that one can simply use the same field realization for several different granular positions. By keeping the c-th realization of decomposed variables $\boldsymbol{\xi}^c$ unchanged, the field realization can be adapted for any configuration of the facets in the discrete model.

Structural strength of a quasibrittle material is typically governed by two important material properties, namely the material strength and fracture energy. Realistic fracture models should therefore incorporate random spatial variability of at least these two variables. It is reasonable to consider the material strength fully correlated with the fracture energy (Grassl and Bažant, 2009). Furthermore, in the proposed lattice model, we also include the shear strength f_s and mode-II fracture energy G_s, which are again assumed to fully be correlated to the tensile strength f_t and mode-I fracture energy G_t, respectively. Assuming identical coefficient of variation (cov), we can use the same realizations of the random field to generate values of material strengths and fracture energies. For X substituted by any of the four mentioned mechanical properties, we can write

$$X(\boldsymbol{x}) = \bar{X}\boldsymbol{H}(\boldsymbol{x}) \tag{7}$$

where $\bar{X}$ stands for mean value of the particular property. The mean value of the (field) random variable H has to equal 1.

In this study, the following parameters of the Weibull-Gauss grafted distribution (Eq. 2a) were used: $m = 24$; $s_1 = 0.486$ MPa; $h_{gr} = 0.364$ MPa; $\delta_G = 0.25$. These values provide overall mean value μ_H=1; standard deviation $\delta_H \approx$0.25 and grafting probability $F_H(h_{gr}) \approx 10^{-4}$. Two correlation lengths d were considered: a shorter length $d_4 = 40$ mm (according to Grassl and Bažant (2009)) and a longer length $d_8 = 80$ mm (according to Vořechovský (2007)). The computation is performed with $N = 24$ realizations of the random field for each correlation length.

4. Simulations of bending of notched beams

The first set of beams (depth $D = 300$ mm, span $S = 2.4D$, thickness $t = 40$ mm) loaded in three-point-bending were modeled with a central notch up to 1/6 of its depth. Ten deterministic simulations were

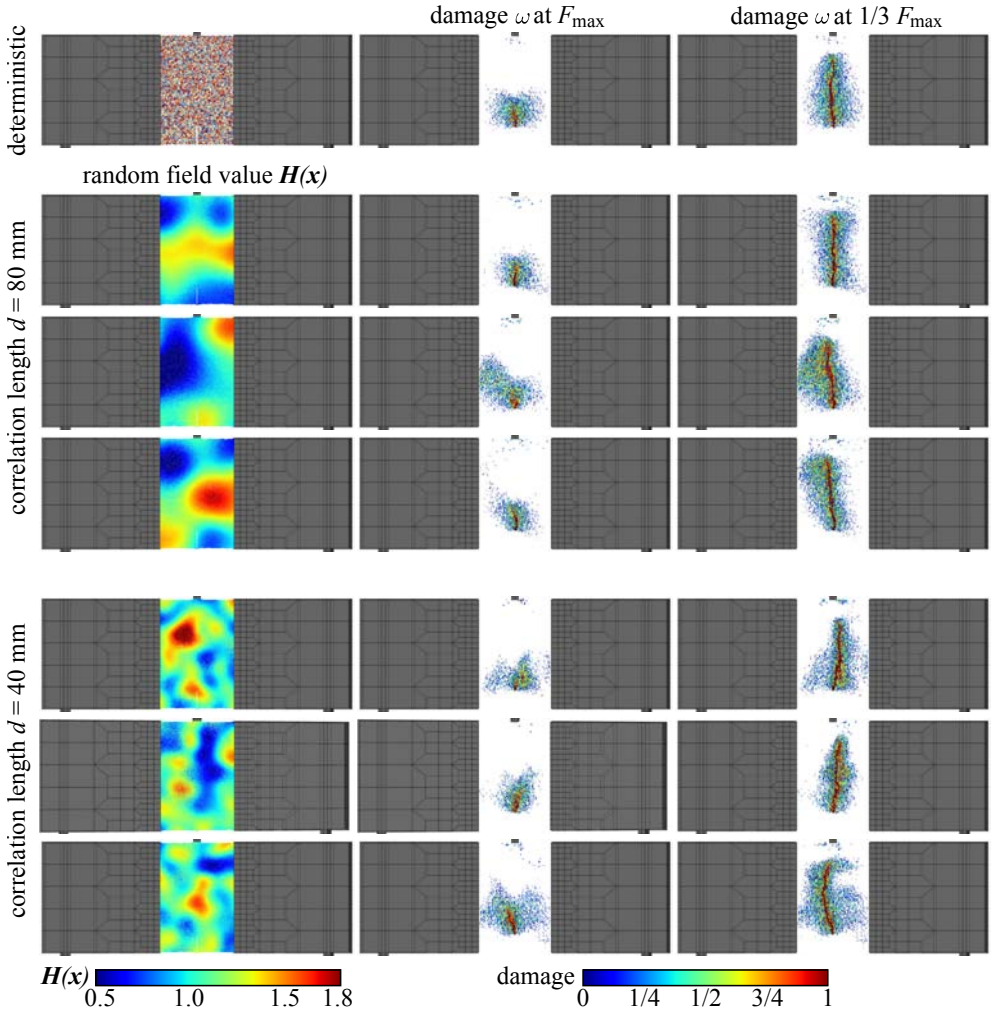

Fig. 4: Realizations of random field $\boldsymbol{H}$ *(left) and corresponding damage patterns developed in bent notched beams at the peak force (middle) and after the load dropped to* $1/3$ *of its maximum (right).*

computed. These simulations exhibit a certain scatter because of the pseudo-random granular positions differing for each realization. For both correlation lengths 40 and 80 mm, 24 simulations with spatial material randomness were performed. All the simulations were terminated when the magnitude of the loading force dropped to 1/3 of the maximal reached load $F_{\max}$. To ensure numerical stability in the presence of softening, the simulations were controlled by prescribing an increase of the crack mouth opening displacement (CMOD) in every step.

The notch present in the model induces a stress concentration at the notch tip. Therefore, high stresses occur only in a small area above the notch tip. Therefore, a crack initiates and propagates always from the notch tip. In stochastic calculations with rather large correlation length, local strength fluctuations within the region of high-stresses diminishes because of the imposed spatial correlation. Thus, the peak load $F_{\max}$ depends mostly on a single value of the random field realization at the notch tip location. In other words, a random field with correlation length greater than the length/width of FPZ can be, in the vicinity of the crack tip, viewed as a random constant – random field becomes a random variable at that region.

The obtained load-deflection curves are shown in Fig. 3. The figure also shows the maximal loads $F_{\max}$ in its upper left corner. The effect of the spatial strength fluctuations on the mean value of maximum load is negligible. The mean value of $F_{\max}$ is, for the deterministic calculation, $\mu_d = 11.3$ kN and, for stochastic simulations with $d = 40$ and 80 mm $\mu_4 = \mu_8 = 11.0$ kN. However, the standard deviations of the peak load are significantly influenced by the material randomness. The standard deviation of deterministic calculations (given solely by random aggregate position) is $\delta_d = 0.4$ kN. Significant increase in the standard deviation is observed for both correlation lengths: $\delta_4 = 1.5$ kN ($d = 40$ mm)

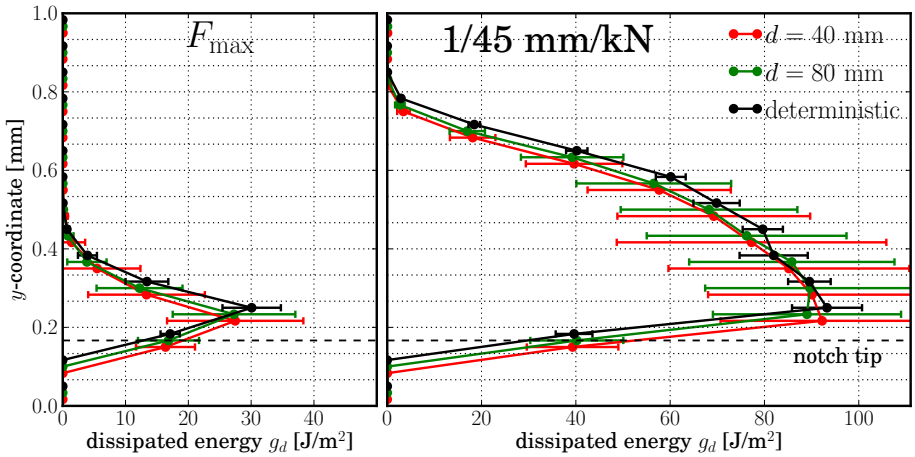

Fig. 5: Energy per unit ligament area g_d dissipated in notched beams up to a) maximal load and b) reference beam compliance $1/45$ mm/kN in dependence on the vertical position in the beam.

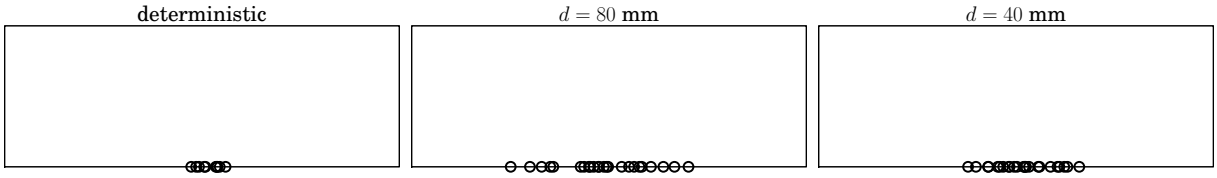

Fig. 6: Points of crack initiation of unnotched beams for various degrees of randomness.

and $\delta_8 = 1.8$ kN ($d = 80$ mm). Since the maximal load of the beam is given by local meso-level strength of a small area above the notch tip, we believe that the fluctuation rate does not influence the standard deviation (unless it is so small that material parameters vary significantly inside the FPZ).

For several selected realizations, the computed damage patterns (damage parameter ω from Eq. 1) at the peak load and at the termination of the simulations are showed in Fig. 4 together with the corresponding random field realization. Even though one can notice that the crack is slightly attracted (repelled) by areas of low (high) strength, the macrocrack trajectory is similar to the deterministic case (dictated by the singular stress field).

In order to compare energy dissipation in the beams, we need to determine simulation stages where the same portion of the ligament has already been damaged. Therefore, we select a stage when equivalent crack lengths (according to LEFM) are equal. Thus, all the models should have at that (reference) stage the same (reference) compliance, chosen as 1/45 mm/kN (Fig. 3). The depth of specimen was divided into horizontal stripes of depth s (Fig. 1c). All the energy dissipated at inter-particle contacts within a specific stripe was summed into variable G_d. One can normalize that energy by ligament area as $g_d = G_d/st$. The mean values and standard deviations of g_d are plotted in Fig. 5 for every stripe at the peak load and at the reference compliance stages. The figure confirms that the mean energy dissipation in notched tests does not change when the spatial material randomness is applied. Similarly to the peak force behavior, standard deviations of dissipated energy increase when randomness is present.

5. Simulations of bending of unnotched beams

The second simulation set focused on bending of unnotched beams where cracks initiate from a smooth bottom surface. Ten deterministic simulations and $N = 24$ simulations with random field for each correlation length were performed. To control the simulation, one needs to find some monotonically increasing variable, here again the CMOD was used. For unnotched beams with spatially fluctuating meso-level strength, the location of the macrocrack and thus the position of the crack mouth is not known in advance. Therefore, several short overlapping intervals were monitored simultaneously and the controlling CMOD was chosen to be the maximum one over them. Note, that other possibility of controlling variable might be the total energy dissipation in the specimen (Gutiérrez, 2004).

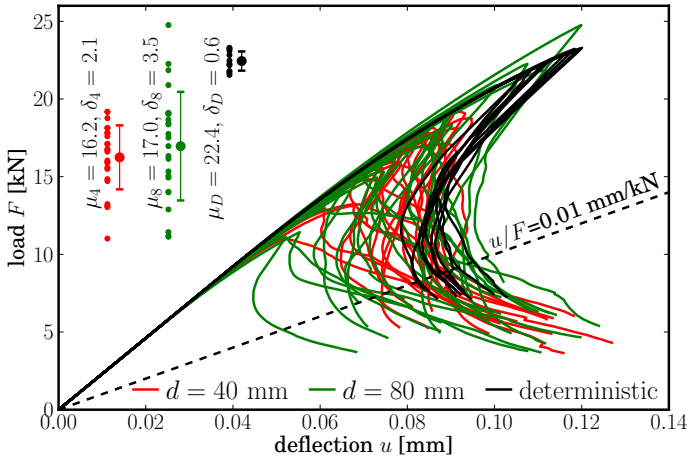

Fig. 7: Load-deflection curves for simulations of TPB beams without notch.

The variations in position of the crack mouth of the macrocrack are documented in Fig. 6. The Figure demonstrates the fundamental difference between notched and unnotched simulations. When no notch is present, the high-level stress region is much larger, located along the bottom central part of the specimen. Material strength and fracture energy fluctuate within the region and allow the macrocrack to "choose a weak spot" to initiate from. The higher is the distance form the midspan, the lower tensile stress appears. In the process of crack(s) formation, the stress field with a certain ability of redistribution increases towards the barrier (randomly varying strength and energy). The crack would start far from the midspan only when the material strength (and energy) of all points closer to the midspan is higher than in the surrounding. It is thus expectable (and confirmed by Fig. 6) that short correlation length, resulting in fluctuations that generate the weak spots more frequently, shrinks the zone where the macrocrack initiates. Indeed, the initiation zone for correlation length $d = 80$ mm is wider than for $d = 40$ mm.

Load deflection curves obtained from all the performed simulations are plotted in Fig. 7. The upper left corner shows the mean values and standard deviations of the peak load $F_{\max}$. The more fluctuating is the local strength, the weaker spot is statistically present and thus the lower is the mean value: $\mu_d = 22.4$ kN (deterministic), $\mu_8 = 17.0$ kN ($d = 80$ mm), $\mu_4 = 16.2$ kN ($d = 40$ mm). The standard deviation of the maximal force is low for the deterministic set, where $\delta_d = 0.6$ kN (cov$_d$=2.7%). For the correlation length 80 mm, it increases rapidly to $\delta_8 = 3.5$ kN (cov$_8$=21%). When the fluctuation rate increases more ($d = 40$ mm), the standard deviation of $F_{\max}$ decreases back to $\delta_4 = 2.1$ kN (cov$_4$=13%). This trend simply comes from the fact that the standard deviation of the local strength in the weakest spot inside some fixed region decreases with decreasing correlation length. Theoretically, the maximal standard deviation of $F_{\max}$ should be obtained for $d \approx \infty$ (a situation when the random field can be represented by a random variable – a random constant over the specimen volume).

Fig. 8 presents several selected realizations of the random field $\boldsymbol{H}$ and the computed damage patterns. One can see that the damage patterns differ for different levels of randomness. In the deterministic case, the damaged region at the peak load stage spans continuously the whole bottom area and the damage intensity directly depends on the distance from the midspan. For a random local strength and local fracture energy, the damage regions are more localized around low random field values. There is usually one such region for correlation length $d = 40$ mm and several low strength regions for $d = 80$ mm.

To compare the energy dissipation, we again choose some reference compliance that marks stages with the same LEFM crack length. The reference compliance now equals to 1/100 mm/kN (Fig. 7). Contrary to results from notched simulations, summation of total energy dissipated in stripes (per unit ligament area) is dependent on material randomness. In Fig. 9, deterministic calculations show higher values of dissipated energy g_d both for the peak force stage and for the stage at the reference compliance. This is caused by two factors: i) the localized macrocrack propagates in stochastic simulations through areas of lower meso-level strength and meso-level fracture energy, thus less energy is dissipated in total; ii) Distributed pre-peak cracking outside the macrocrack occurs mostly for deterministic simulation and thus it increases its total energy dissipation. Note that from about the middle of the specimens depth

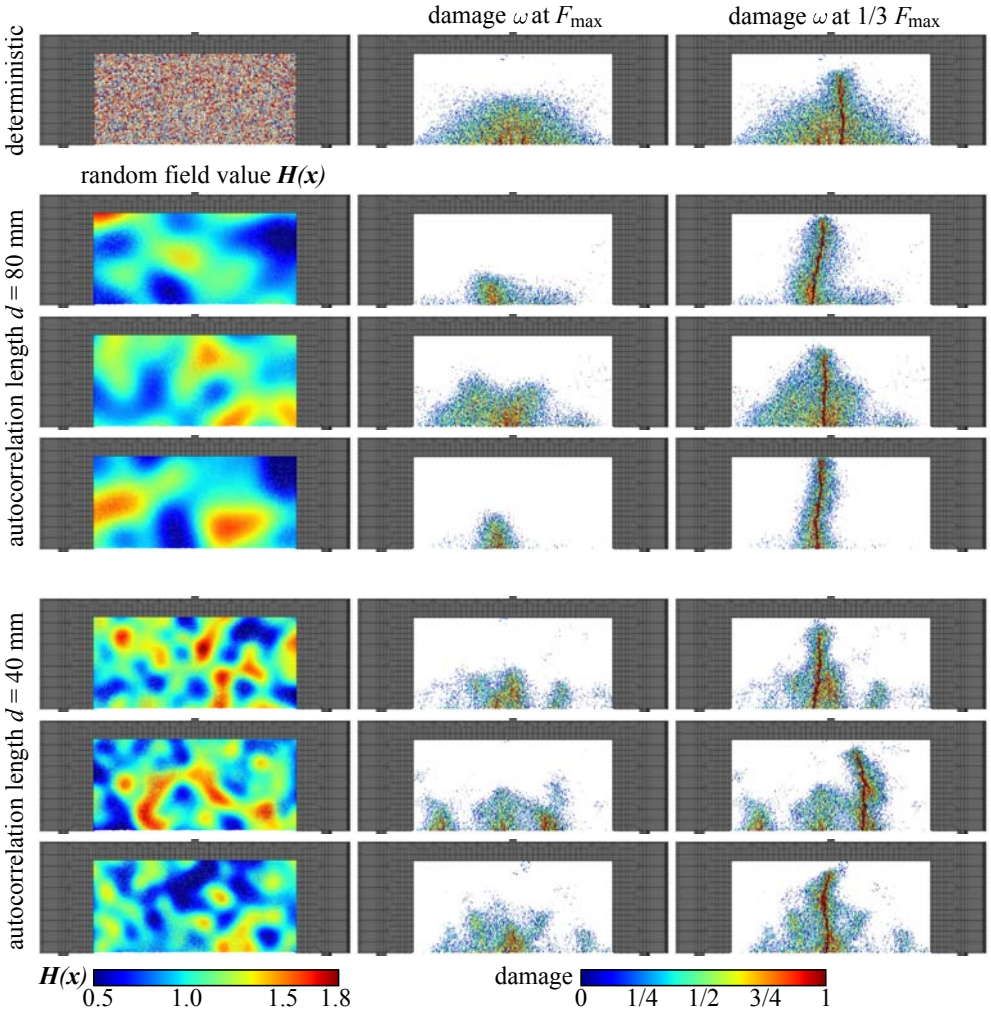

Fig. 8: Realizations of random field $\boldsymbol{H}$ *(left) and corresponding damage patterns developed in bent beams without notch at the peak force (middle) and after the load dropped to* $1/3$ *of its maximum (right).*

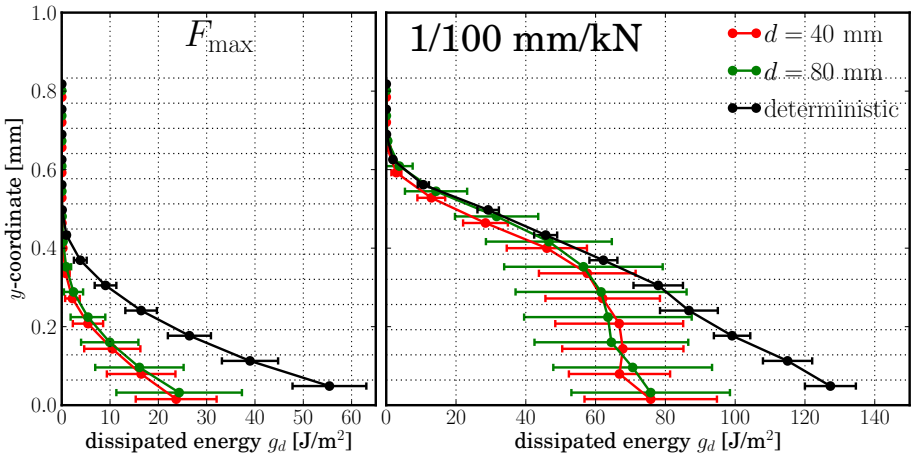

Fig. 9: Energy per unit ligament area dissipated in unnotched beams up to a) maximal load and b) reference beam compliance $1/100$ mm/kN *in dependence on vertical position in the beam.*

upwards, the energy dissipation of deterministic and stochastic simulations again match each other. This is because the crack at that depth cannot choose the weak region as it has already localized and the stress field forces the crack to grow from the current crack tip; and no pre-peak distributed cracking takes place there.

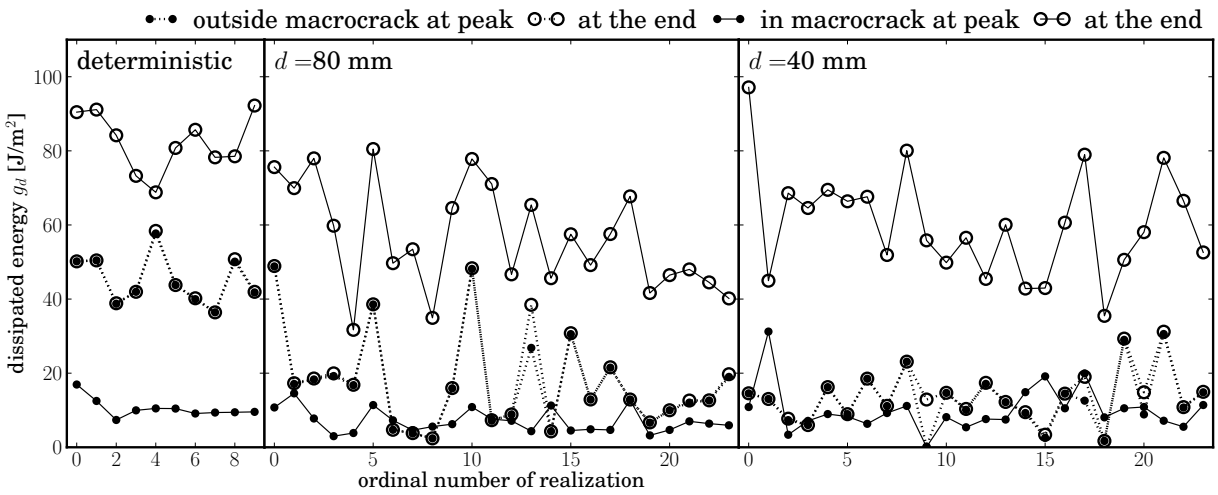

Fig. 10: Energy dissipation inside and outside the macro-crak at the peak load and at the reference compliance stages for every simulation.

Finally, we focus on a deeper analysis of the energy dissipation along the bottom surface. In the bottom boundary stripe of width $2d_{\max} = 19$ mm, the dissipated energies (per unit ligament area) inside and outside the macrocrack were evaluated for stages at the peak load and at the reference compliance. These values are plotted in Fig. 10 separately for each simulation. The results document that distributed cracking outside macrocrack in the most bottom layer after the peak is reached is close to zero. The amount of energy dissipated *outside* a macrocrack is much higher for the deterministic simulations than for those with random fields. Some of the simulations for $d = 80$ mm reached the value of the deterministic model, which can be explained by an absence of a locally weak spot and subsequent extensive pre-peak distributed cracking (see Fig. 8, third row). The energy dissipated *inside* the macrocrack at the reference compliance is clearly higher in the deterministic case than in the stochastic one. This is due to the positive correlation of local meso-level energy and meso-level strength at the inter-particle bonds. Since the macrocrack propagates through locally weaker areas, it also dissipates less energy there. Aspects related to correlation between the local tensile strength and fracture energy have been discussed by Vořechovský and Novák (2004).

6. Conclusions

We analyzed the influence of material spatial randomness on the peak load and the energy dissipation using a discrete lattice-particle model that reflects the concrete meso-scopic structure, i.e. the aggregate composition. The spatial material randomness was introduced by simultaneous scaling of the local meso-level strength and fracture energy of inter-particle bonds by realizations of autocorrelated random field. Two basic cases of three-point-bent beams were investigated: i) beams with a notch and ii) beams without a notch (the modulus of rupture test). Numerical results generally confirm theoretical expectations.

It has been found that:

- for the simulation with a sufficiently deep notch, the crack is forced to start at the notch tip. Therefore, the mean value of the maximal load for notched beam simulations does not change when material spatial randomness applies. However, the standard deviation of the maximal load increases when strength randomness is introduced. Also, the energy dissipation in deterministic and random media exhibit the same mean but an increasing standard deviation for the random cases.

- In the case of unnotched beams, the macrocrack initiates in a locally weaker spot.When a shorter correlation length of material properties is applied, the weaker is statistically the initiation spot and therefore the mean of the maximal load is lower. Standard deviations of the maximal load increase when randomness applied, however the shorter correlation lengths lead to a decrease of the standard deviation.

- Energy dissipated in unnotched beams is dependent on the randomness of the material. Two effects responsible for the dependency were identified. i) Change of the dissipated energy due to correlation of the local meso-level fracture energy and low meso-level strength of inter-particle bonds through which the macrocrack propagates. Depending on the sign of the energy-strength cross-correlation, this effect may increase or decrease the dissipated energy. For the current settings of the model, the lower is the local meso-level strength, the lower is also the local fracture energy and the lower is the energy dissipated inside the macrocrack. ii) The pre-peak distributed cracking has a tendency to localize only in weaker areas and thus the material dissipated less energy outside the macrocrack when random field is applied.

Acknowledgments

The financial support received from the Czech Science Foundation under Project No. P105/11/P055 and the Ministry of Education, Youth and Sports of the Czech Republic under Project No. LH12062 is gratefully acknowledged.

References

Alava, M. J., Nukala, P. K. V. V., and Zapperi, S. (2006). Statistical models of fracture. *Advances in Physics*, Vol. 55, No. 3-4, pp. 349–476.

Barenblatt, G. I. (1962). Mathematical theory of equilibrium cracks in brittle fracture. *Advances in Applied Mechanics*, Vol. 7, pp. 55–129.

Bažant, Z. P., and Jirásek, M. (2002). Nonlocal integral formulations of plasticity and damage: Survey of progress. *ASCE's Journal of Engineering Mechanics*, Vol. 128, No. 11, pp. 1119–1149.

Bažant, Z. P., Le, J.-L., and Bazant, M. Z. (2009). Scaling of strength and lifetime distributions of quasibrittle structures based on atomistic fracture mechanics. *Proceeding of the National Academy of Sciences, USA*, Vol. 106, No. 28, pp. 11484–11489.

Bažant, Z. P., and Novák, D. (2000). Probabilistic nonlocal theory for quasibrittle fracture initiation and size effect. I. Theory. *ASCE's Journal of Engineering Mechanics*, Vol. 126, No. 2, pp. 166–174.

Bažant, Z. P., and Pang, S.-D. (2007). Activation energy based extreme value statistics and size effect in brittle and quasibrittle fracture. *Journal of the Mechanics and Physics of Solids*, Vol. 55, pp. 91–131.

Bažant, Z. P., and Planas, J. (1998). *Fracture and size effect in concrete and other quasibrittle materials.* CRC Press.

Bažant, Z. P., and Xi, Y. (1991). Statistical size effect in quasi-brittle structures: II. Nonlocal theory. *ASCE's Journal of Engineering Mechanics*, Vol. 117, No. 7, pp. 2623–2640.

Bolander, J. E., and Saito, S. (1998). Fracture analyses using spring networks with random geometry. *Engineering Fracture Mechanics*, Vol. 61, pp. 569–591.

Cusatis, G., Bažant, Z., and Cedolin, L. (2003). Confinement-shear lattice model for concrete damage in tension and compression: I. theory. *ASCE's Journal of Engineering Mechanics*, Vol. 129, pp. 1439–1448.

Cusatis, G., Bažant, Z., and Cedolin, L. (2006). Confinement-shear lattice csl model for fracture propagation in concrete. *Computer Methods in Applied Mechanics and Engineering*, Vol. 195, pp. 7154–7171.

Cusatis, G., and Cedolin, L. (2007). Two-scale study of concrete fracturing behaviour. *Engineering Fracture Mechanics*, Vol. 6, pp. 3–17.

Eliáš, J., and Bažant, Z. (2011). Fracturing in concrete via lattice-particle model. In Onate, E., and Owen, D., editors, *2nd international conference on particle-based methods - fundamentals and applications*, p. 12, Barcelona, Spain. CD ROM.

Grassl, P., and Bažant, Z. P. (2009). Random lattice-particle simulation of statistical size effect in quasi-brittle structures failing at crack initiation. *ASCE's Journal of Engineering Mechanics*, Vol. 135, pp. 85–92.

Grassl, P., and Rempling, R. (2008). A damage-plasticity interface approach to the meso-scale modelling of concrete subjected to cyclic compressive loading. *Engineering Fracture Mechanics*, Vol. 75, pp. 4804–4818.

Gutiérrez, M. A. (2004). Energy release control for numerical simulations of failure in quasi-brittle solids. *Communications in Numerical Methods in Engineering*, Vol. 20, No. 1, pp. 19–29.

Hillerborg, A., Modéer, M., and Petersson, P.-E. (1976). Analysis of crack formation and crack growth in concrete by means of fracture mechanics and finite elements. *Cement and Concrete Research*, Vol. 6, pp. 773–782.

HongShuang, L., ZhenZhou, L., and XiuKai, Y. (2008). Nataf transformation based point estimate method. *Chinese Science Bulletin*, Vol. 53, No. 17, pp. 2586–2592.

Li, C.-C., and Kiureghian, A. D. (1993). Optimal discretization of random fields. *ASCE's Journal of Engineering Mechanics*, Vol. 119, No. 6, pp. 1136–1154.

Van Mier, J. G. M., and Van Vliet, M. R. A. (2003). Influence of microstructure of concrete on size/scale effects in tensile fracture. *Engineering Fracture Mechanics*, Vol. 70, pp. 2281–2306.

Vořechovský, M., and Novák, D. (2004). Modeling statistical size effect in concrete by the extreme value theory. In Walraven, J., Blaauwendaad, J., Scarpas, T., and Snijder, B., editors, *5^{th} International Ph.D. Symposium in Civil Engineering, held in Delft, The Netherlands*, Vol. 2, pp. 867–875, London, UK. A.A. Balkema Publishers. ISBN 90 5809 676 9.

Vořechovský, M. (2007). Interplay of size effects in concrete specimens under tension studied via computational stochastic fracture mechanics. *International Journal of Solids and Structures*, Vol. 44, pp. 2715–2731.

Vořechovský, M. (2008). Simulation of simply cross correlated random fields by series expansion methods. *Structural Safety*, Vol. 30, pp. 337–363.

Vořechovský, M. (2010). Incorporation of statistical length scale into weibull strength theory for composites. *Composite Structures*, Vol. 92, No. 9, pp. 2027–2034.

Vořechovský, M., and Novák, D. (2009). Correlation control in small-sample monte carlo type simulations i: A simulated annealing approach. *Probabilistic Engineering Mechanics*, Vol. 24, pp. 452–462.

Vořechovský, M., and Sadílek, V. (2008). Computational modeling of size effects in concrete specimens under uniaxial tension. *International Journal of Fracture*, Vol. 154, pp. 27–49.

Weibull, W. (1939). The phenomenon of rupture in solids. In *Royal Swedish Institute of Engineering Research*, Vol. 153, pp. 1–55, Stockholm.